Supplementary Information: Na vs Li Metal Anodes For Batteries: Unraveling Thermodynamic and Electronic Origins of Voids and Developing Descriptors for Artificial Surface Coatings

Victor Venturi,* Rodrigo Freitas, and Iwnetim Iwnetu Abate*

Department of Materials Science and Engineering, Massachusetts Institute of Technology, Cambridge, Massachusetts 02139, USA

E-mail: vventuri@mit.edu; iabate@mit.edu

Details on Capillary Fluctuation Theory (CFT)

The CFT model expresses the surface free energy of a quasi-two-dimensional periodic surface slab ($b \ll W$) as

$$E = b \int_0^W \gamma(\theta) ds, \tag{S.1}$$

where b is the thickness of the slab, W is the its length, γ is the surface energy, θ is the angle between the interface normal and the nominally flat normal direction, and ds is an infinitesimal arc length along the ribbon interface. This can be seen in Figure S1, which compares the flat, un-relaxed surface, with the rough, relaxed one. The arc length can be approximated as

$$ds = \sqrt{(dx)^2 + (dh)^2} = \sqrt{1 + \left(\frac{dh}{dx}\right)^2} dx = \sqrt{1 + [h'(x)]^2} dx \approx \left(1 + \frac{[h'(x)]^2}{2}\right) dx \tag{S.2}$$

We also know that $^{dh}/_{dx} = \tan\theta \approx \theta$ for small values of θ. Additionally, a Taylor expansion of $\gamma(\theta)$ around $\theta_0 = 0$ (flat surface) yields

$$\gamma(\theta) = \gamma_0 + \gamma_0' \theta + \frac{1}{2}\gamma_0'' \theta^2 \tag{S.3}$$

Combining Equations S.2 and S.3 into Equation S.1, we can express

$$\begin{aligned} E &= b \int_0^W \left(\gamma_0 + \gamma_0' \theta + \frac{1}{2}\gamma_0'' \theta^2\right) \left(1 + \frac{\theta^2}{2}\right) dx \\ &= b \int_0^W \left[\gamma_0 + \gamma_0' \theta + \frac{1}{2}\left(\gamma_0 + \gamma_0''\right)\theta^2 + \frac{\gamma_0' \theta^3}{2} + \frac{\gamma_0'' \theta^4}{4}\right] dx \end{aligned}$$

Since θ is assumed to be small, we can neglect the higher order terms dependent on θ^3 and θ^4. Additionally, because this integral is conducted on a system with periodic boundary conditions, the integral from boundary to boundary of $\theta = h'(x)$ is equal to 0, since $h(0) =$

$h(W)$. Therefore, the change in energy from a flat to a rough surface can be expressed as

$$\Delta E = E - bW\gamma_0 = \frac{b}{2}\left(\gamma_0 + \gamma_0''\right)\int_0^W \theta^2 dx = \frac{b}{2}\left(\gamma_0 + \gamma_0''\right)\int_0^W \left[h'(x)\right]^2 dx \tag{S.4}$$

In this expression, the term $S = \gamma_0 + \gamma_0''$ is the interfacial stiffness, and represents the energy penalty factor associated with perturbing the surface away from a pure flat profile.[1–3] Therefore, the larger the value of stiffness, the more difficult it is for a flat surface to become rougher. In order to estimate the value of S, Hoyt et al.[1] proposed to decompose the height profile $h(x)$ as a Fourier series:

$$h(x) = \sum_k A_k e^{ikx} \tag{S.5}$$

From the equipartition theorem, the free energy E_k of each mode (which contains two degrees of freedom, namely, $\sin(kx)$ and $\cos(kx)$) must be equal to $k_B T$, where k_B is Boltzmann's constant and T is the temperature (usually the melting point for solid-liquid interfaces).[1] Therefore, the following relationship arises:

$$\langle |A_k|^2 \rangle = \frac{k_B T}{bW\left(\gamma_0 + \gamma_0''\right)k^2} \tag{S.6}$$

This expression allow us to extract the values of stiffness from the MD simulations of the ribbon-like surface slabs by simply measuring the slope of the line which fits $\langle |A_k|^2 \rangle^{-1}$ plotted against k^2.[1–3]

Following the procedures from previous works,[1–3] the values of Li and Na lattice parameters at different temperatures were used to create quasi-two-dimensional surface slabs for the (100), (110), and (111) surface facets, which were then subsequently simulated in LAMMPS for 1,000 ps at a time step of 0.0025 ps. This guaranteed that the snapshots of the final 500 ps of simulation were fully converged, and could be used for the capillary fluctuation analysis. For each slab, a vacuum of at least 40 Å was used. The binning procedure established by Brown et al.[2] was employed to extract the height profiles of the simulated slabs, as shown

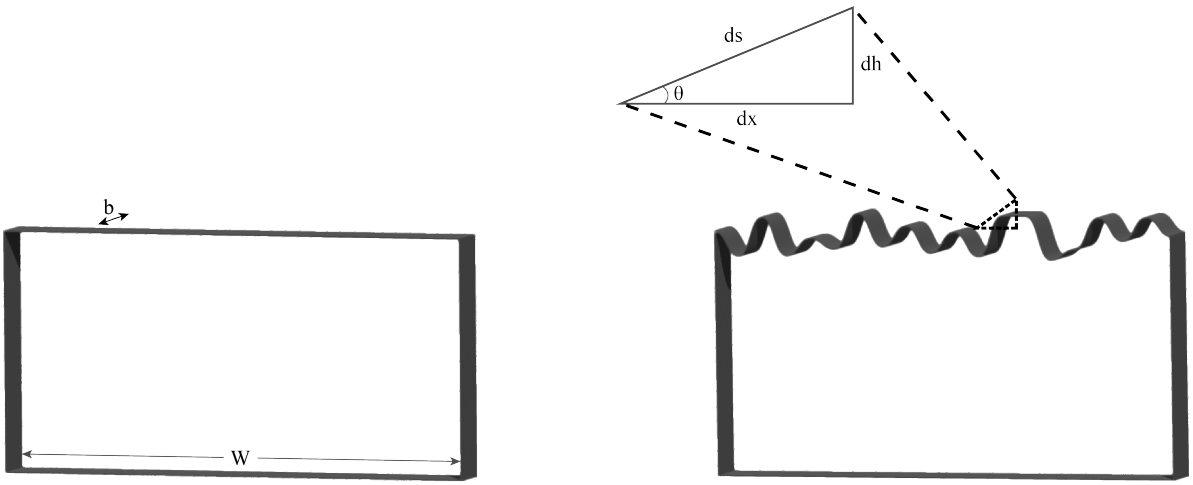

Figure S1: Example of **(a)** flat, unrelaxed and **(b)** rough, relaxed surface slabs. Note that the slabs are ribbon-like, with $b \ll W$. The inset denotes an infinitesimal element of the surface of the slab, used to compute the relationship between infinitesimal terms dx, dh, ds, and θ.

in Figure S2.

For each interface, the surface profiles of the last 500 ps of simulation were decomposed into their respective Fourier modes, and used to evaluate the relationship between $\langle |A_k|^2 \rangle$ and k^2, as shown in Figure S3. For estimation of the interfacial stiffness at different temperatures, the slope of the fitted lines shown in Figure S3 was used. Note that, for large wavenumbers, the surface fractals deviate from linear trends, since the fluctuation wavelengths are comparable to the lattice parameter and the capillary relationship breaks down. [2] Therefore, in order to adequately evaluate the stiffness of the different facets, we limited the fitting to wavenumber that correspond to at least four lattice parameters of fluctuation periodicity. Furthermore, since, for lower temperatures, deviations from linearity start occurring even at smaller wavenumbers, we investigated all linear fits using a subset of wavenumbers, from smallest to largest, and chose a cutoff when the slope change dramatically (by more than 10%). An example of this is seen in Figure S4.

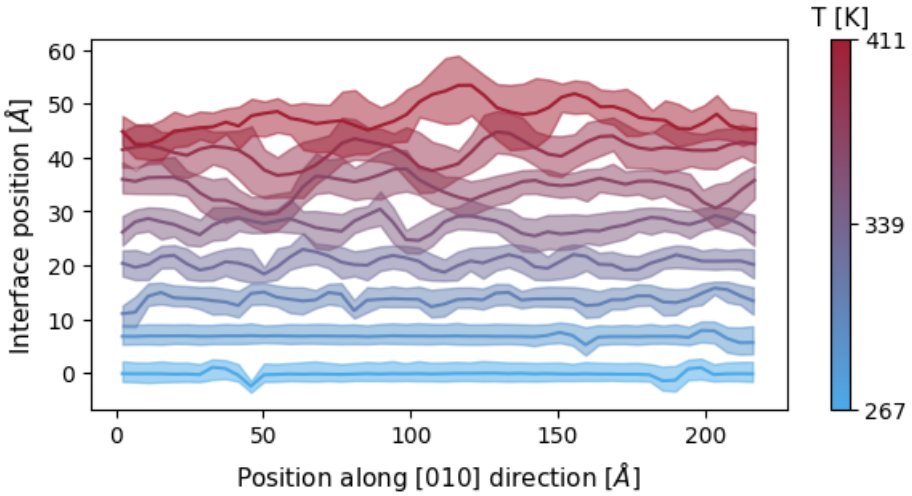

Figure S2: Example of average (001) Na surface profiles at different temperatures. Values along the y-axis are relative only. Shaded areas correspond to 95% confidence intervals.

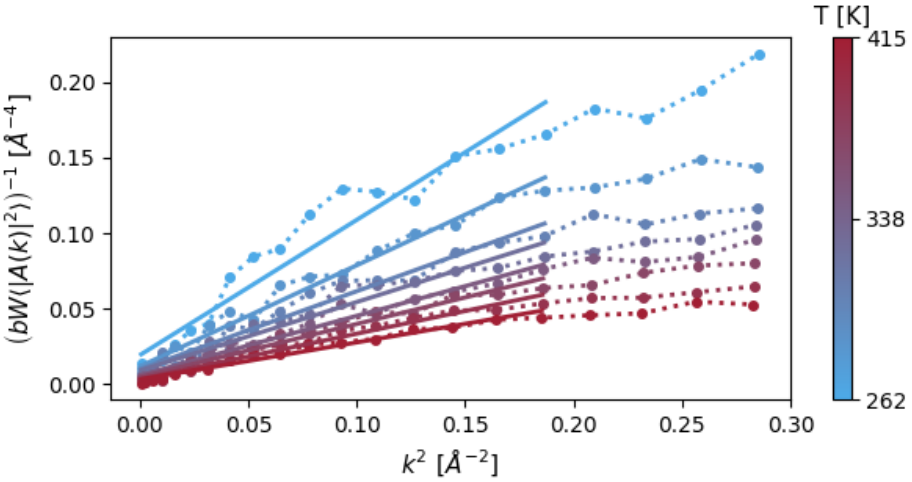

Figure S3: Example of correlation between $(bW\langle|A|^2\rangle)^{-1}$ and k^2 for Li (110) slab at different temperatures.

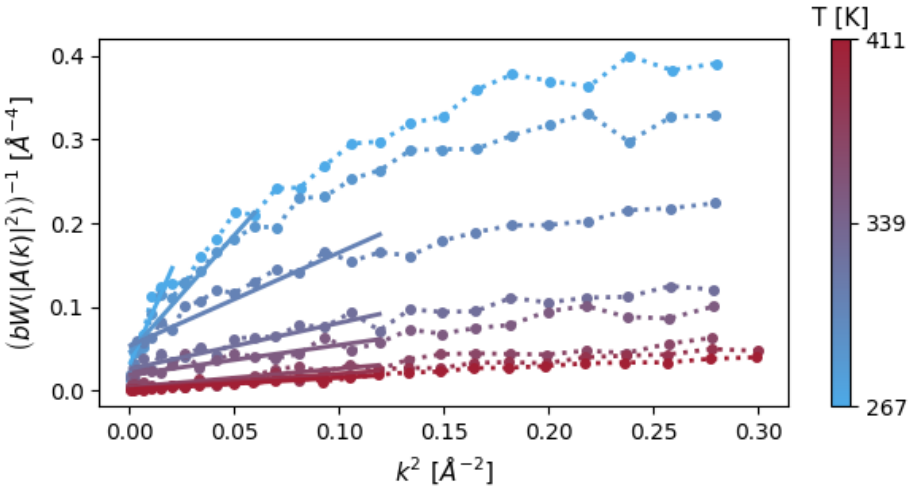

Figure S4: Example of how, for different temperatures, different $\langle|A_k|^2\rangle^{-1} \times k^2$ fits were used for a Na (110) surface slab.

Alkali Properties from Molecular Dynamics Simulations

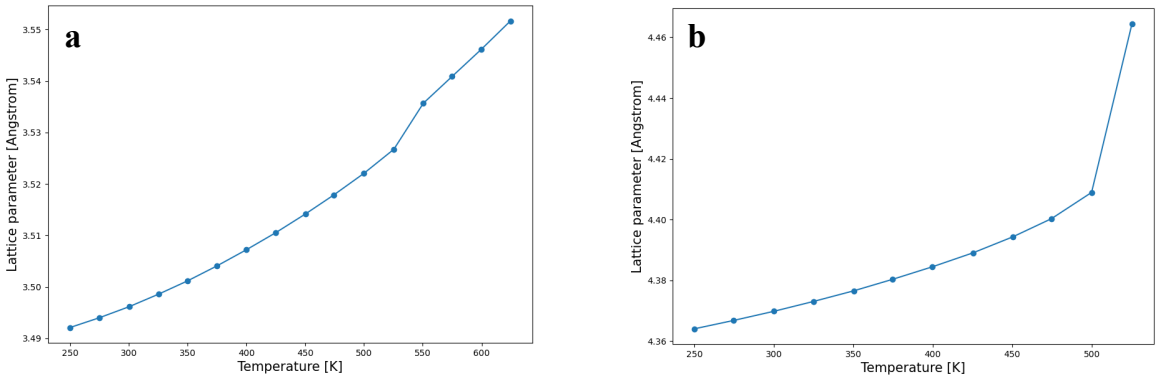

Figure S5: Plots showing the relationship between lattice parameter and temperature for **(a)** Li and **(b)** Na.

Structures in Density Functional Theory Simulations

In the Figures S7 and S8 below, we show examples of the interface structures used in DFT simulations prior and post relaxation. It is clear that, in cases of strong interactions between Na atoms in the metallic slab and F atoms in the SEI material, the ground state system is characterized by large structural distortions.

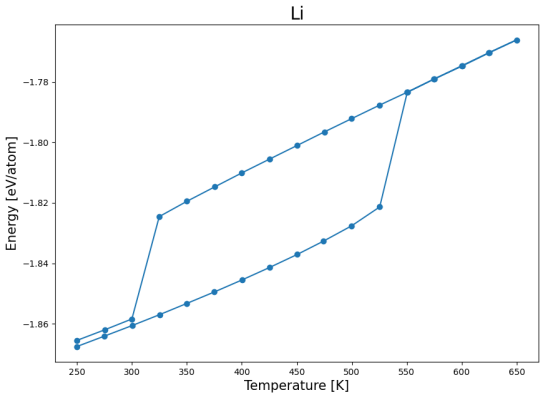

Figure S6: Plot of energy per atom versus temperature for a bulk Li system, demonstrating hysteresis.

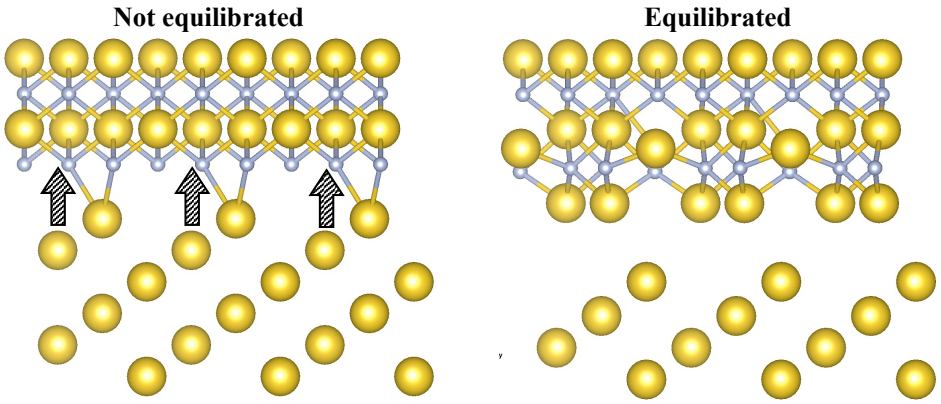

Figure S7: Strong interactions between Na atoms in metallic (111) slab and F atoms in NaF (111) structure highly deform the morphology of the sodium surface

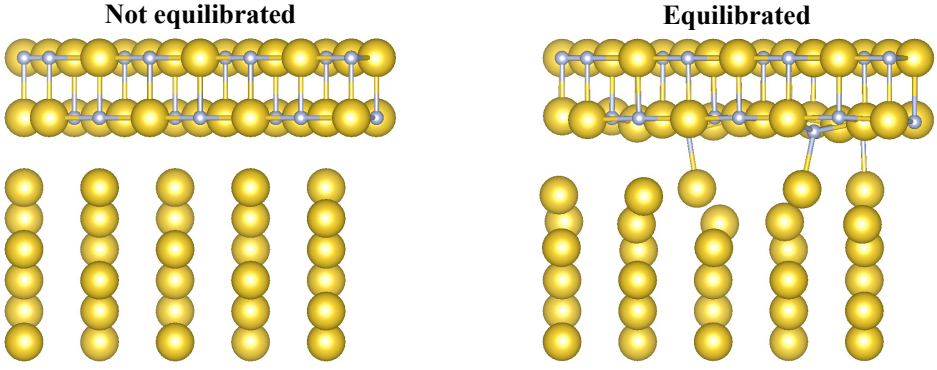

Figure S8: Weaker, and more spread out, interactions between Na(111) and NaF(100) do not significantly alter the surface of the sodium slab, allowing it to retain similar parameters as those from the isolated slab calculations

The values of adhesion energies for the several interfaces we studied. The adhesion energy is calculate as:

$$E_{\text{adhesion}} = \frac{E_{\text{interface}} - (E_{\text{alkali slab}} + E_{\text{SEI slab}})}{\text{interface area}} \tag{S.7}$$

Note, however, that, for these calculations, we did not conduct DFT calculations of the isolated strained slabs, but only of the unstrained surfaces. Therefore, imbued in the values of adhesion we report are the strain energy terms associated with the deformations needed to create coherent interfaces; hence, we refer to these values as approximate adhesion energies in the main text. The comparison between Ω (both $\Omega^{(11)}$ and $\Omega^{(12)}$) and adhesion energy for each interface is shown in Figure S9. For interfaces with Li, there appears to be some correlation between adhesion energy and Ω, as found in previous studies:[4–6] systems with lower E_{adhesion} (corresponding to more favorable interface formation, compared to isolated slabs) tend to exhibit lower values of Ω, and, thereby, lower values of the critical temperature at which vacancies become soluble among occupied sites. However, for Na, such correlation is not present, indicating that adhesion energy may not be an appropriate descriptor for the thermodynamics of vacancy congregation for Na metal/SEI interfaces.

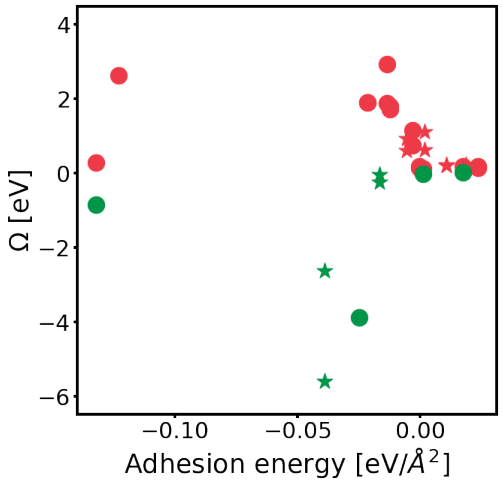

Figure S9: Values of Ω versus approximate adhesion energies of the interfaces in this study. Stars denote interfaces with Li metal, and circles, with Na metal. Red indicates thermodynamic tendency for vacancy accumulation, while green indicates resistance to this phonomenon. There appears to be some correlation between adhesion energy and Ω for Li, as noted in previous studies,[4–6] but the same cannot be said for Na interfaces.

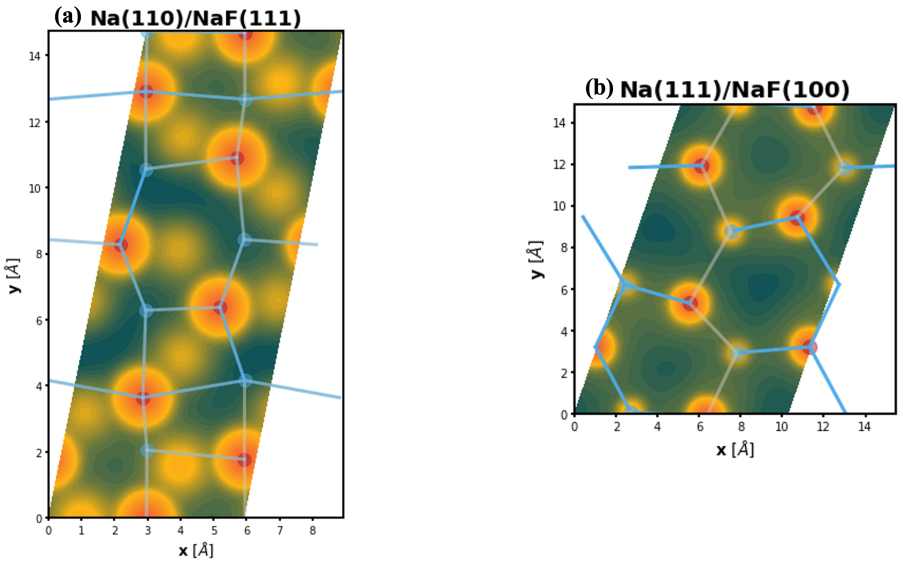

Figure S10: Contour plots of the logarithm (base 10) of the integrated charge density at the top-most Miller plane of the Na-slabs. Red and circles indicate positions of Na atoms of type tag1 and tag2, respectively, while straight lines denote the relative $\epsilon_{VV}^{(12)}$ interactions, with darker, more opaque lines representing stronger interactions. Interfaces represented are **(a)** Na(110)/NaF(111) and **(b)** Na(111)/NaF(100). Some of the lines that appear absent are represented through their periodic images.

Three ways of summarizing the electronic interactions between coating and anode slab were considered. The first, denoted by $\Delta\chi_{max}$, corresponds to the difference in electronegativities between the most electronegative element of the coating material, and that of the alkali metal: $\Delta\chi_{max} = \chi_{max}^{coat.} - \chi^{alkali}$. The second is related solely to the SEI material, $\Delta\chi_{polar}^{SEI}$, and is a measure of how polarized (and, in consequence, polorizing) the SEI is: $\Delta\chi_{polar}^{SEI} = \chi_{max}^{coat.} - \chi_{min}^{coat.}$. Finally, we also considered the different in the average electronegativity of the SEI material and that of the alkali metal, $\Delta\chi_{avg.} = \chi_{avg.}^{coat.} - \chi^{alkali}$. Methods for quantifying the relative geometries of the interfacing materials are explained in the main text.

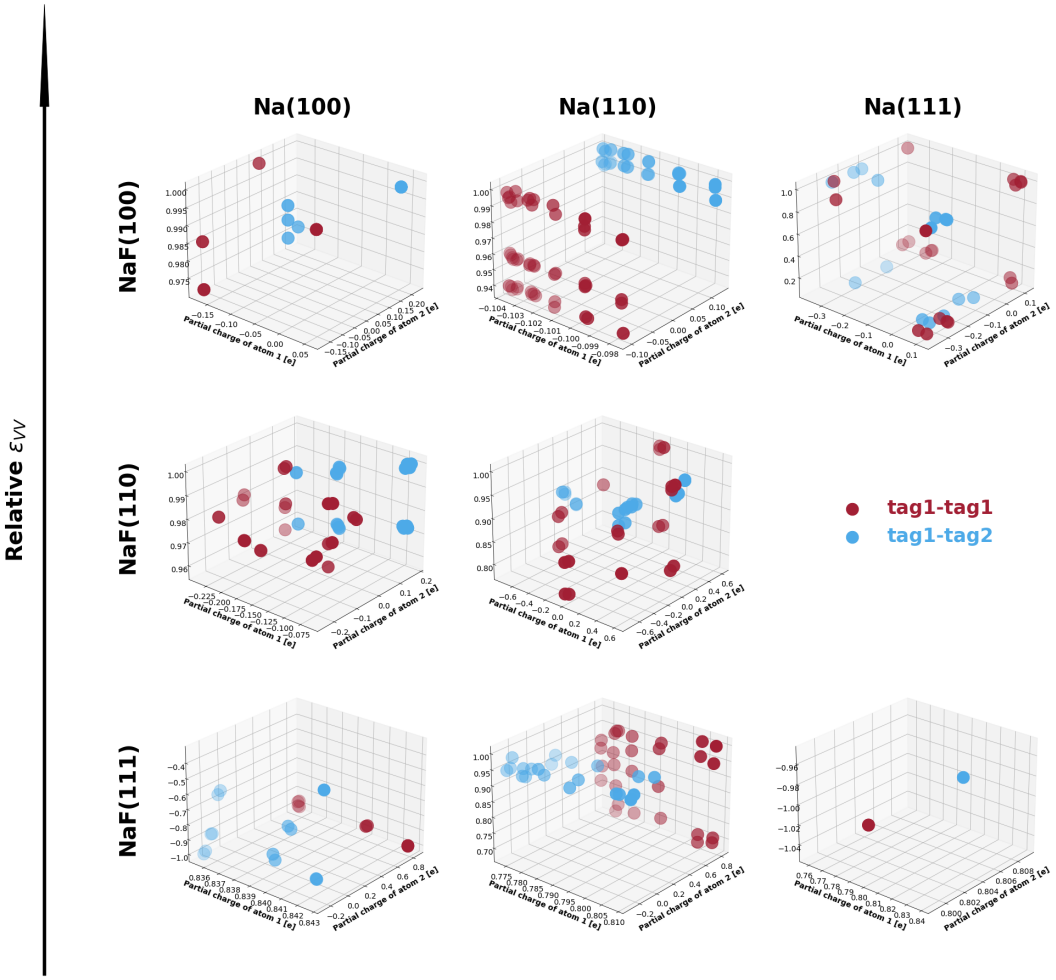

Figure S11: Relationship between relative ϵ_{VV} parameter (for species solely on the top-most, tag1-tag1, and between the two top-most, tag1-tag2, Miller planes) and partial charge (in units of the elementary charge $\sim 1.6 \times 10^{-19}$ C) of the respective atom. Partial charge of atom 1 always refers to the atom of type tag1, while the other axis refers to the other interacting atom, regardless if it is of type tag1 or tag2. Parameter data has been normalized by the maximum value for purposes of consistent visualization. While variations in the ϵ_{VV} are observed, they are not as strongly correlated to the partial charge as those of the ϵ_{VO} parameter.

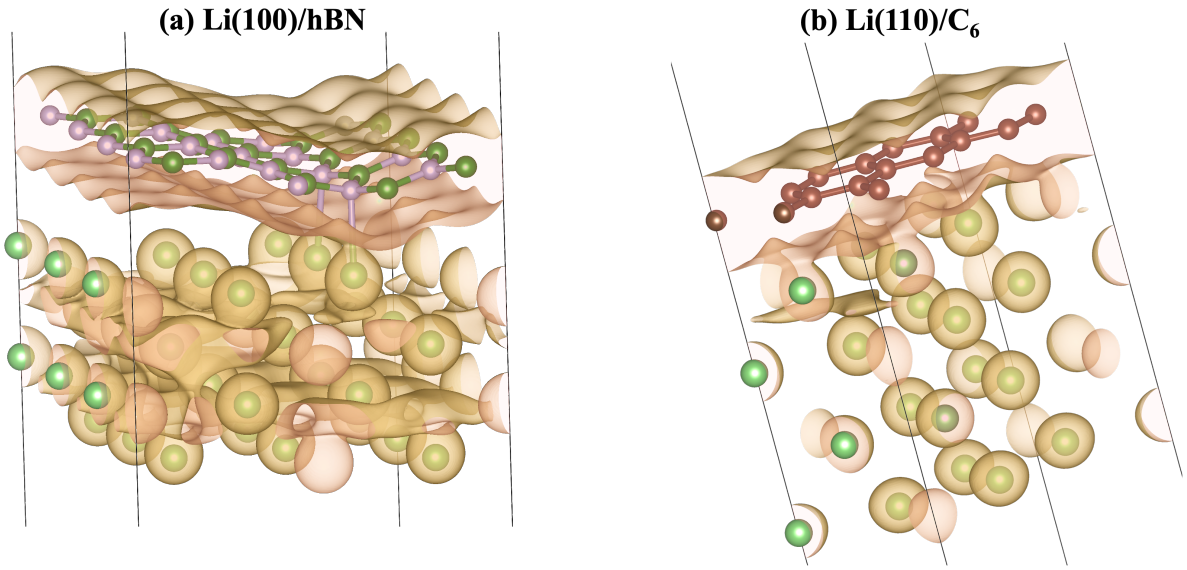

Figure S12: Isosurfaces of charge density for two example Li/2D systems: **(a)** Li(100)/hBN and **(b)** Li(110)/C_6 . As can be seen, sections of the metallic electron cloud, which are not centered on a Li atom, can exhibit large heterogeneity in their spatial distribution. This can lead to misleading Bader charge attributions.

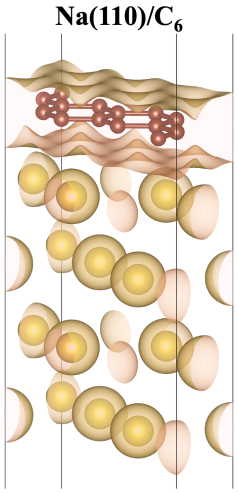

Figure S13: Isosurfaces of charge density for Na(110)/C_6 system. The electronic density is highly homogeneous in this interface, indicating no interactions between the two participant materials

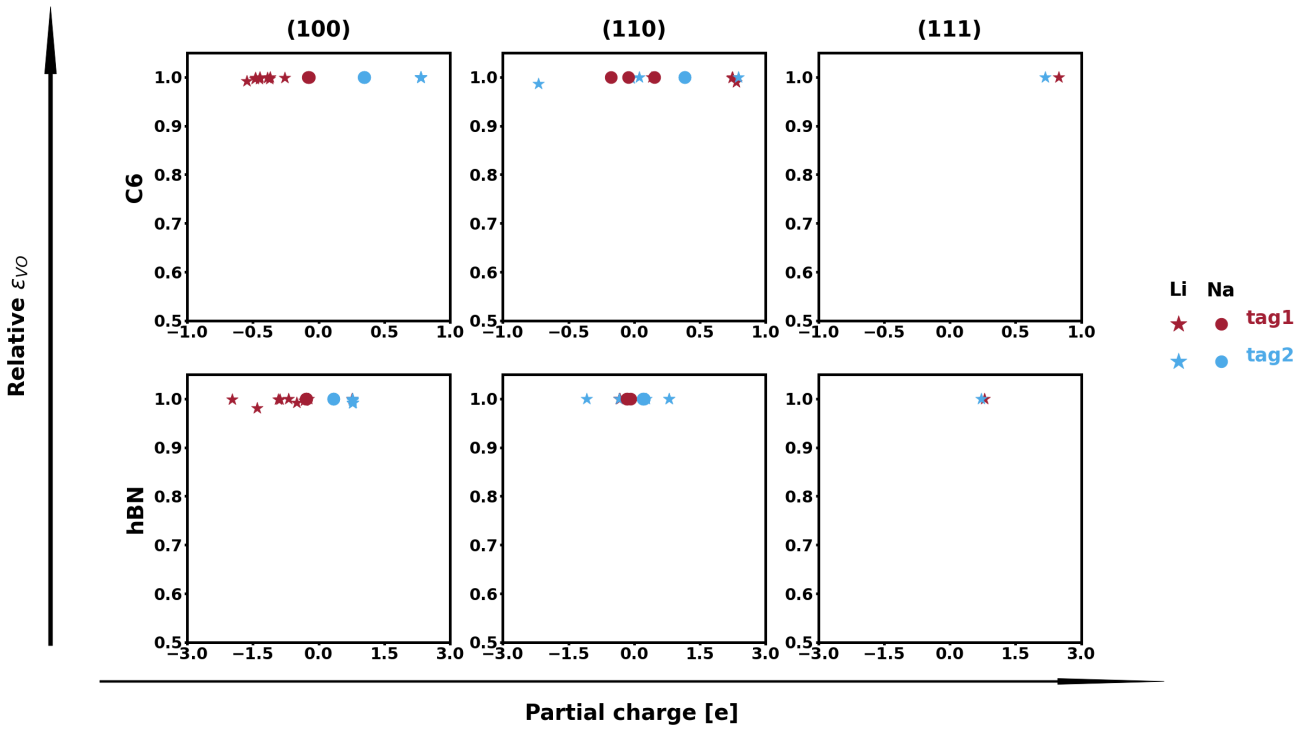

Figure S14: Relationship between relative ϵ_{VO} parameter (for species on the top-most, tag1, and second top-most, tag2, Miller planes) and partial charge (in units of the elementary charge $\sim 1.6 \times 10^{-19}$ C) of the respective atom for alkali/2D interfaces. Parameter data has been normalized by the maximum value for purposes of consistent visualization. In most cases, variations in the value of this parameter are highly correlated with the partial charge.

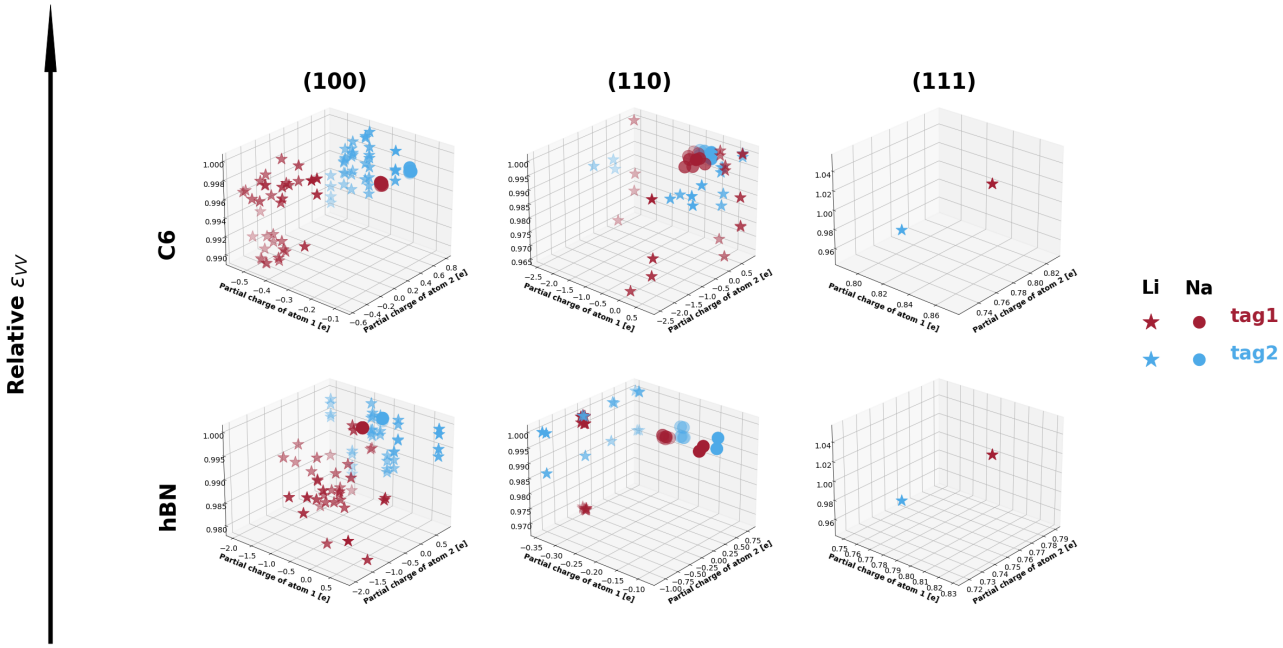

Figure S15: Relationship between relative ϵ_{VV} parameter (for species solely on the top-most, tag1-tag1, and between the two top-most, tag1-tag2, Miller planes) and partial charge (in units of the elementary charge $\sim 1.6 \times 10^{-19}$ C) of the respective atom for alkali/2D interfaces. Partial charge of atom 1 always refers to the atom of type tag1, while the other axis refers to the other interacting atom, regardless if it is of type tag1 or tag2. Parameter data has been normalized by the maximum value for purposes of consistent visualization.

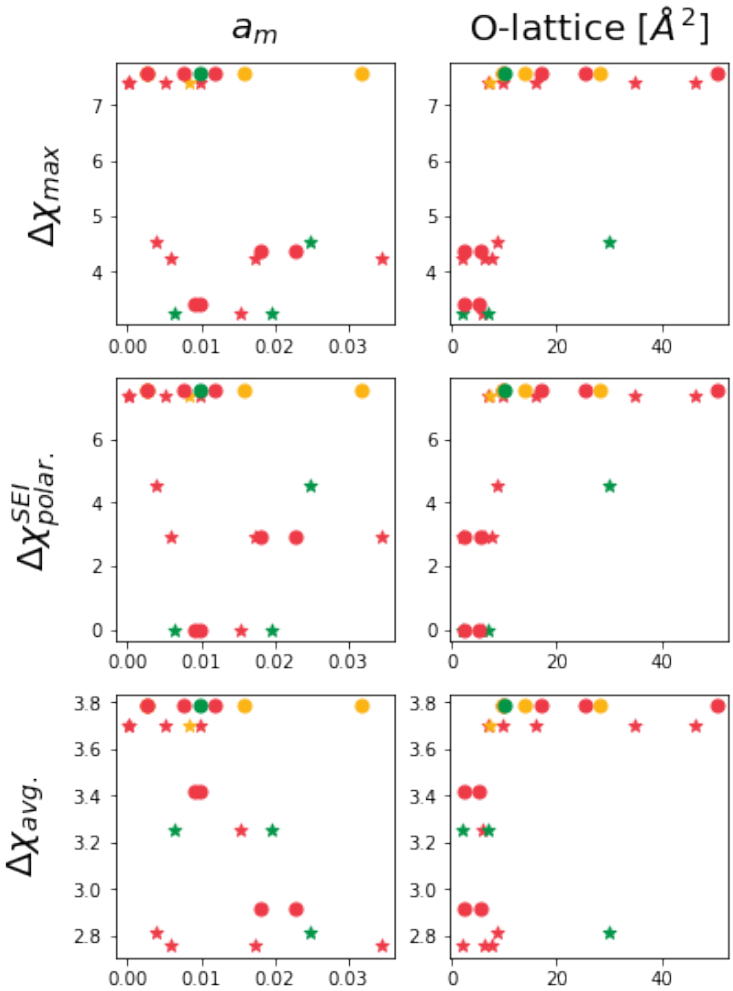

Figure S16: Comparison between electronic interactions and geometries of several interfaces. Mulliken electronegativities are measured in eV. Circles indicate Na interfaces, and stars, Li interfaces. Red corresponds to systems that are not resistant to vacancy accumulation, green to system that are resistant, yellow to systems that are partially resistant, and grey, to systems that have not been investigated

Theoretical Battery Studies Checklist[7]

Manuscript Title:	Survey of Interfaces for Enabling Metallic Anodes in Lithium and Sodium Batteries
Submitting Authors*:	Victor Venturi, Rodrigo Freitas, Iwnetim Abate

#	Question	Y/N/NA†
1	Have you provided all assumptions, theory, governing equations, initial and boundary conditions, material properties, e.g., open circuit potential (with appropriate precision and literature sources), constant states, e.g., temperature, etc.? **Remarks:** All assumptions have either been explicitly written, or are clearly presented in the provided references.	Y
2	If the calculations have a probabilistic component (e.g. Monte Carlo, initial configuration in Molecular Dynamics, etc.), did you provide statistics (mean, standard deviation, confidence interval, etc.) from multiple (≥ 3) runs of a representative case? **Remarks:** There are no probabilistic components in our methodology.	NA
3	If data-driven calculations are performed (e.g. Machine Learning), did you specify dataset origin, the rationale behind choosing it, what all information does it contain and the specific portion of it being utilized? Have you described the thought process for choosing a specific modeling paradigm? **Remarks:** No data driven techniques were employed in this work.	NA
4	Have you discussed all sources of potential uncertainty, variability, and errors in the modeling results and their impact on quantitative results and qualitative trends? Have you discussed the sensitivity of modeling (and numerical) inputs such as material properties, time step, domain size, neural network architecture, etc. where they are variable or uncertain? **Remarks:** We provide sources of uncertainty and discuss the sensitivity of the results to the inputs.	Y
5	Have you sufficiently discussed new or not widely familiar terminology and descriptors for clarity? Did you use these terms in their appropriate context to avoid misinterpretation? Enumerate these terms in the 'Remarks'. **Remarks:** We include equations and definitions to any term with which a reader may not be familiar. Additionally, we list several references to other work that can also provide additional clarification to any of the employed methodology.	Y

* I verify that this form is completed accurately in agreement with all co-authors, to the best of my knowledge.

† Y ≡ the question is answered completely. Discuss any N or NA response in 'Remarks'.

References

(1) Hoyt, J. J.; Asta, M.; Karma, A. Method for Computing the Anisotropy of the Solid-Liquid Interfacial Free Energy. *Phys. Rev. Lett.* **2001**, *86*, 5530–5533, DOI: 10.1103/PhysRevLett.86.5530.

(2) Brown, N. T.; Martinez, E.; Qu, J. Solid-Liquid Metal Interface Definition Studies Using Capillary Fluctuation Method. *Computational Materials Science* **2019**, *168*, 65–73, DOI: 10.1016/j.commatsci.2019.05.059.

(3) Saidi, P.; Freitas, R.; Frolov, T.; Asta, M.; Hoyt, J. J. Free Energy of Steps at Faceted (111) Solid-Liquid Interfaces in the Si-Al System Calculated Using Capillary Fluctuation Method. *Computational Materials Science* **2017**, *134*, 184–189, DOI: 10.1016/j.commatsci.2017.03.044.

(4) Venturi, V.; Viswanathan, V. Thermodynamic Analysis of Initial Steps for Void Formation at Lithium/Solid Electrolyte Interphase Interfaces. *ACS Energy Lett.* **2022**, 1953–1959, DOI: 10.1021/acsenergylett.2c00550.

(5) Yang, C.-T.; Qi, Y. Maintaining a Flat Li Surface during the Li Stripping Process via Interface Design. *Chem. Mater.* **2021**, *33*, 2814–2823, DOI: 10.1021/acs.chemmater.0c04814.

(6) Yang, M.; Mo, Y. Interfacial Defect of Lithium Metal in Solid-State Batteries. *Angewandte Chemie International Edition* **2021**, *60*, 21494–21501, DOI: 10.1002/anie.202108144.

(7) Mistry, A. et al. A Minimal Information Set To Enable Verifiable Theoretical Battery Research. *ACS Energy Lett.* **2021**, *6*, 3831–3835, DOI: 10.1021/acsenergylett.1c01710.